

A STUDY OF FAR INFRARED CAVITY AT -3.6° GALACTIC LATITUDE

B. B. Sapkota and B. Aryal

Journal of Nepal Physical Society

Volume 5, Issue 1, October 2019

ISSN: 2392-473X

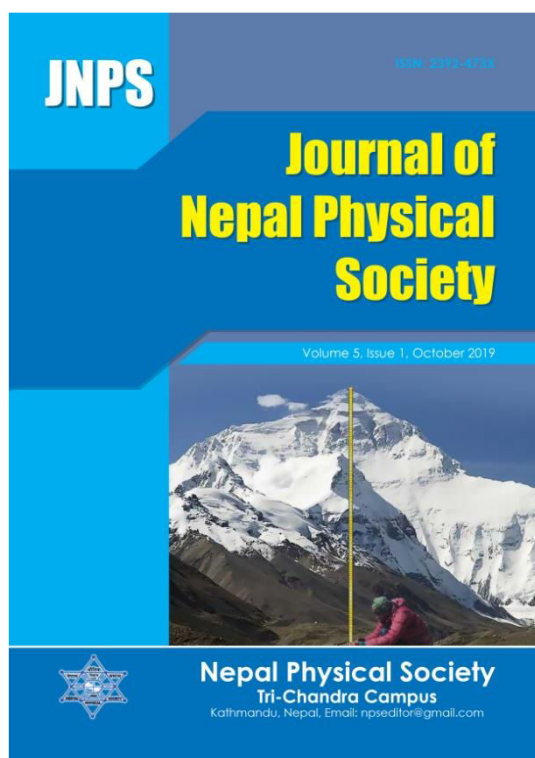
Editors:

Dr. Vinaya Kumar Jha

Dr. Binod Adhikari

Dr. Kapil Adhikari

JNPS, 5 (1), 54-58 (2019)



Published by:

Nepal Physical Society

P.O. Box: 2934

Tri-Chandra Campus

Kathmandu, Nepal

Email: npseditor@gmail.com



A STUDY OF FAR INFRARED CAVITY AT -3.6^0 GALACTIC LATITUDE

B. B. Sapkota^{1,2*} and B. Aryal²

¹Mahendra Ratna Campus, Tahachal, Tribhuvan University, Kathmandu, Nepal

²Central Department of Physics, Tribhuvan University, Kirtipur, Nepal

*Corresponding Email: bhanusapkota45@gmail.com

ABSTRACT

We have present properties like inclination angle, dust color temperature and dust mass of core region in far infrared located nearby White dwarf WD2236+541. The size of cavity is $0.84 \text{ pc} \times 0.51 \text{ pc}$. The cavity is formed by high pressure at the time of white dwarf formation. The dust color temperature varies from 22.42 K to 27.43 K. The inclination angle of cavity is 54.2^0 . The position of white dwarf is found at R.A. J (2000) = $22^{\text{h}}38^{\text{m}}24^{\text{s}}$ and Dec. J (2000) = $+54^{\circ}26^{\text{m}}19^{\text{s}}$.

Key words: White dwarf, Dust color temperature, Dust mass, Inclination angle, Cavity

INTRODUCTION

White dwarf is formed during death stage of star. When the star runs out of its nuclear fuel, the density in the interior increases, but temperature does not change much. The electrons become degenerate, and pressure is mainly due to pressure of degenerate electron gas and pressure due to the ions. White dwarfs have no internal source of energy, but further gravitational contraction is prevented by the pressure of the degenerate electron gas. The white dwarf has mass of the order of 0.6 to $1.4M_{\text{sun}}$ but whose sizes is approximately that of Earth. The average density of white dwarf is $1.4 \times 10^9 \text{ kgm}^{-3}$ [1, 2].

By studying Polytrophic behaviour the temperature, mass, density and pressure inside the white dwarf varies $R^{-2.5}$, R^{-3} , R^{-6} and R^{-10} respectively, where R represents radius of white dwarf. Also the radius of a white dwarf decreases as its mass increases [9]. In the present work, we discuss inclination angle, the color temperature, and dust mass of core region of White dwarf WD2236+541.

THEORY AND METHOD

Inclination Angle:

The inclination angle is given by Holmberg (1946) formula [8]

$$\cos^2 i = \frac{\left(\frac{b}{a}\right)^2 - q^2}{1 - q^2}$$

Where, a = major diameter

b = minor diameter

q = intrinsic flatness = 0.2

Dust color temperature Estimation:

We use data base from the IRAS $60 \mu\text{m}$ and $100 \mu\text{m}$ flux densities is similar to that of Schnee *et al.* [4]. By knowing the flux densities at $60 \mu\text{m}$ and $100 \mu\text{m}$, the temperature contribution due to dust color can be calculated. The dust temperature T_d in each pixel of a FITS image can be obtained by assuming that the dust in a single beam is isothermal and that the observed ratio of $60 \mu\text{m}$ to $100 \mu\text{m}$ emission is due to black body radiation from dust grains at T_d , modified by a power law of spectral emissivity index. The flux density of emission at a wavelength λ_i is given by

$$F_i = \left[\frac{2hc}{\lambda_i^3 \left(e^{\frac{hc}{kT_d}} - 1 \right)} \right] N_d \alpha \lambda_i^{-\beta} \Omega_i \dots \dots \dots (1)$$

where, N_d is the column density of dust grains, is a constant which relates the flux with the optical depth of the dust, β is the spectral emissivity index, and Ω_i is the solid angle subtended at λ_i by the detector. Following [6], we use the equation

$$\beta = \frac{1}{\delta + \omega T_d} \dots \dots \dots (2)$$

to describe the observed inverse relationship between temperature and emissivity spectral index.

Here, δ and ω are free parameters found that the temperature dependence of the emissivity index fits very well with the hyperbolic approximating function.

Considering temperature as an independent variable, the best fit gives $\delta = 0.40 \pm 0.02$ and $\omega = 0.0079 \pm 0.0005 K^{-1}$, with the $\chi^2/\text{degree of freedom} = 120/120$. With the assumptions that the dust emission is optically thin at $60 \mu\text{m}$ and $100 \mu\text{m}$ and that $\Omega_{60} \cong \Omega_{100}$ (true for IRAS image), we can write the ratio ‘‘R’’ of the flux densities at $60 \mu\text{m}$ and $100 \mu\text{m}$ as

$$R = 0.6^{-(3+\beta)} \frac{e^{\frac{144}{T_d}} - 1}{e^{\frac{240}{T_d}} - 1} \dots\dots\dots (3)$$

The value of β depends on dust grain properties as composition, size, and compactness. For reference, a pure blackbody would have $\beta = 0$, the amorphous layer-lattice matter has $\beta \sim 1$, and the metals and crystalline dielectrics have $\beta \sim 2$. For a smaller value of T_d , 1 can be dropped from both numerator and denominator of equation and it takes the form

$$R = 0.6^{-(3+\beta)} \frac{e^{\frac{144}{T_d}}}{e^{\frac{240}{T_d}}} \dots\dots\dots (4)$$

Taking natural logarithm on both sides of equation (4) we find the expression for the temperature as

$$T_d = -96 \frac{1}{\ln\{R \times 0.6^{(3+\beta)}\}} \dots\dots\dots (5)$$

where R is given by

$$R = \frac{F(60 \mu\text{m})}{F(100 \mu\text{m})} \dots\dots\dots (6)$$

$F(60 \mu\text{m})$ and $F(100 \mu\text{m})$ are the flux densities at $60 \mu\text{m}$ and $100 \mu\text{m}$, respectively. In this way we can use equation (5) for the determination of the dust grain temperature [6].

Mass Estimation

The dust masses are estimated from the IR flux densities. In order to estimate the dust masses from the infrared flux densities at $100 \mu\text{m}$, following the calculation of Young *et. al.*[7]. The blackbody intensity can be calculated using the basic expression as given in equation (2). The resulting dust mass depends on the physical and chemical properties of the dust grains, the adopted dust temperature T_d and the distance D to the object.

$$M_{\text{dust}} = \frac{4}{3} \frac{a\rho}{Q_v} \left[\frac{F_v D^2}{B(v,T)} \right] \dots\dots\dots (7)$$

Where a, ρ, Q_v and s_v represent weighted grain size, grain density, grain emissivity and flux density of the region of interest, respectively.

Here, $F_v = f \times 5.288 \times 10^{-9} \text{ MJy/Sr}$

The distance (D) to the cavity is 195 pc, known from the Collaborators [5].

The Planck’s function is given by,

$$B(v, T) = \frac{2hv^3}{c^2} \left[\frac{1}{e^{\frac{hv}{kT}} - 1} \right] \dots\dots\dots (8)$$

Where $h, c, v,$ and T represent Planck's constant, velocity, frequency of light and average temperature of region respectively.

By using, $a=0.1 \mu\text{m}$ [5], $\rho=3000 \text{ kgm}^{-3}$, and $Q_v=0.0010$ for $100 \mu\text{m}$ and 0.0046 for $60 \mu\text{m}$ respectively [6], the expression (7) takes the form :

$$M_{\text{dust}} = 0.4 \left[\frac{F_v D^2}{B(v,T)} \right] \dots\dots\dots (9)$$

We use the equation (9) for the calculation of the dust mass

RESULTS AND DISCUSSIONS

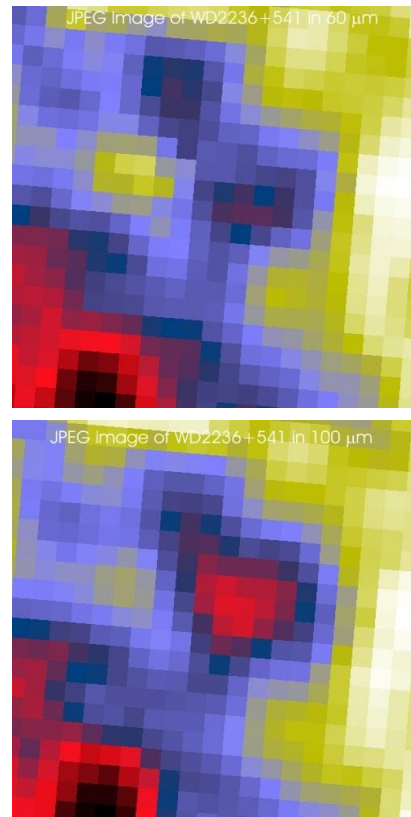


Fig. 1: $0.5^0 \times 0.5^0$ image of the region centered at R.A. (J2000)=22^h 38^m 24^s, Dec. (J2000)=+54^o26^m 19^s at 60 μm (upper) and 100 μm (lower) of WD 2236+541.

In Figure (1), black color near the centre of pixel represents minimum relative flux density and white color at the outer region represents maximum relative flux density in both $60\mu\text{m}$ and $100\mu\text{m}$ wave length.

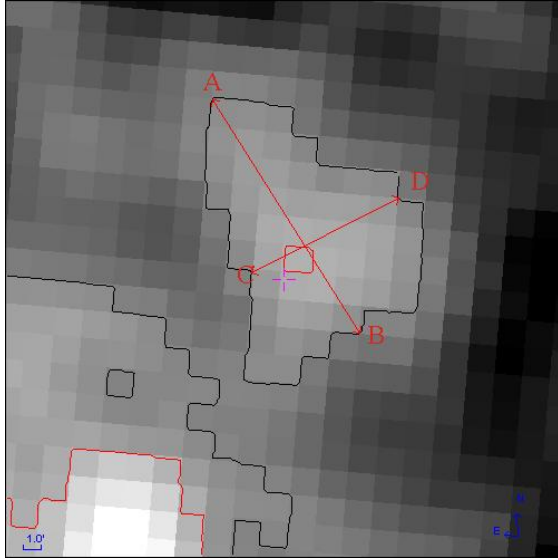


Fig. 2: Cavity formed by $0.5^{\circ} \times 0.5^{\circ}$ image of the region centered at R.A.(J2000)= $22^{\text{h}} 38^{\text{m}} 24^{\text{s}}$, Dec.(J2000)= $+54^{\circ} 26^{\text{m}} 19^{\text{s}}$ at $100\mu\text{m}$ of WD 2236+541. AB and CD line represents major and minor diameter respectively inside the cavity formed within is contour level 122.

In figure (2), + sign represents position of White dwarf. The major and minor diameters are drawn through the region of minimum flux density.

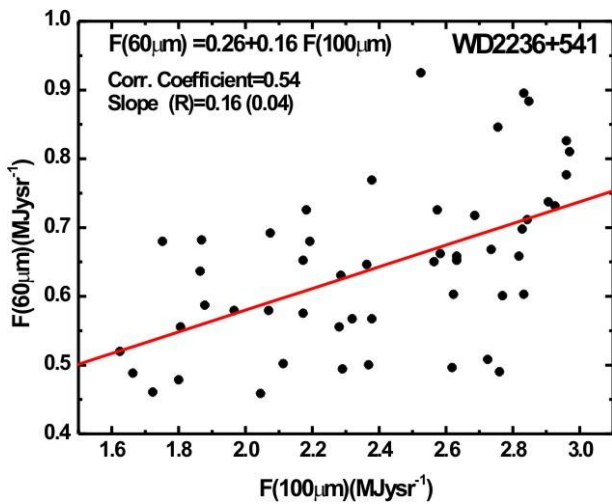


Fig. 3: Scatter plot of $F(60\mu\text{m})$ versus $F(100\mu\text{m})$. The equation of straight line, correlation coefficient, and slope of line are given. In slope the bracket represents the standard error.

Figure (3) represents linear plot of flux density at $60\mu\text{m}$ with $100\mu\text{m}$. The correlation coefficient of straight is 0.54. It indicates a moderate positive linear relationship between $F(60\mu\text{m})$ and $F(100\mu\text{m})$. Also the slope of the line is 0.16.

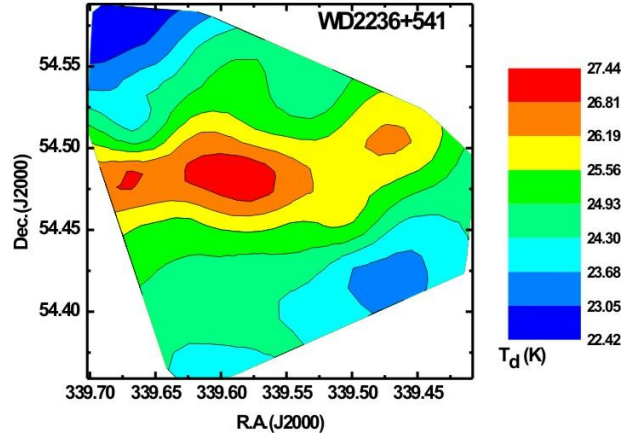


Fig. 4: Contour map of dust color temperature. The blue colour and red colour indicates minimum and maximum temperature respectively.

Figure (4) represents two dimensional contour plots with projection of temperature in XY plane. The maximum temperature is at the centre of region (i.e. red color) and minimum temperature in the outer region (i.e. blue color).

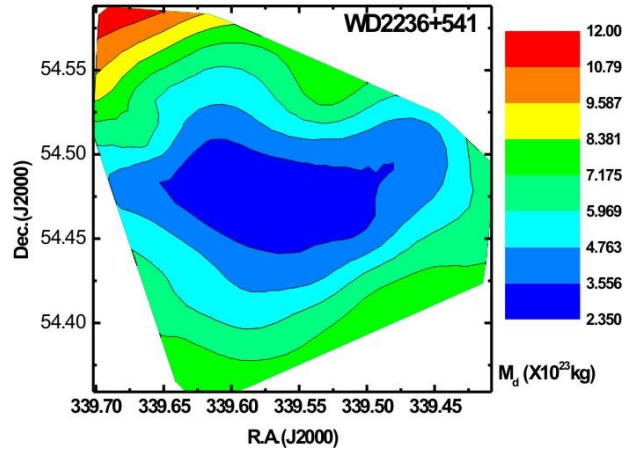


Fig. 5: Contour map of dust mass. The blue colour and red colour indicates minimum mass and maximum mass respectively.

Figure (5) represents two dimensional contour plot with projection of mass in XY plane. The minimum mass is at the centre of region (i.e. blue color) and maximum mass is in the outer region at lower R.A. and higher Dec. (i.e. red color). Comparing figure

(4) and figure (5) it is observed that the minimum temperature region generally has a higher mass and vice versa.

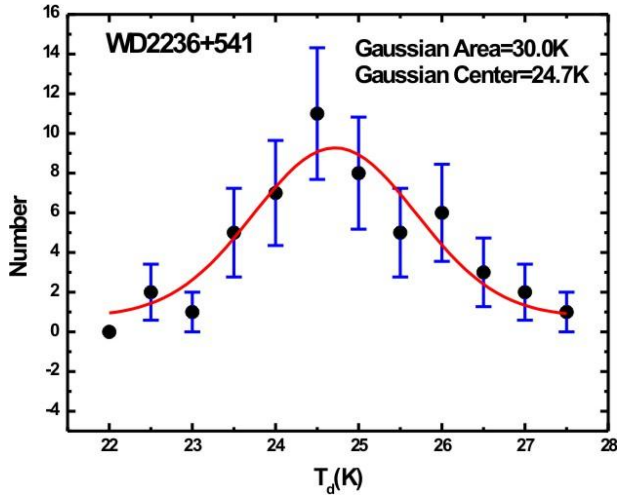


Fig. 6: Distribution of dust color temperature. The red solid curve indicates the Gaussian line and Gaussian parameters are given. The $\pm 1\sigma$ statistical error bars (i.e. blue) are shown. Also $\sigma = \sqrt{n}$.

In figure (6), the horizontal axis represents the values of temperature and vertical axis represents the probability of occurrence of temperature. The probability of occurrence is greater at the centre. The Gaussian centre for temperature is found to be 24.7 K. The dust colour distribution obeys gaussian distribution which indicates that the cavity is in thermal equilibrium.

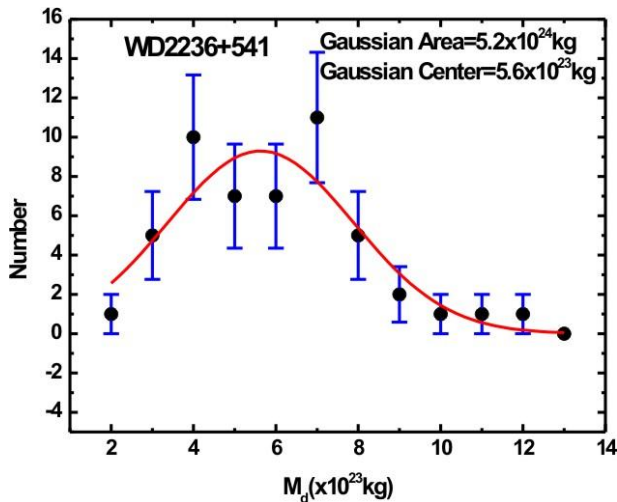


Fig.7: Distribution of dust mass. The red solid curve represents the Gaussian line and Gaussian parameters are given. The $\pm 1\sigma$ statistical error bars (i.e. blue) are shown. Also $\sigma = \sqrt{n}$.

In figure (7), the horizontal axis represents the values of mass and vertical axis represents the probability of occurrence of mass. The probability of occurrence is greater at the centre. The Gaussian area for mass is found to be 5.27×10^{24} kg. The distribution of mass does not fit with Gaussian and the positive skewness in the plot is found to be possibly due to some nearby external sources (i.e. Pulsar, Supernova explosion etc)

CONCLUSIONS

The maximum and minimum dust color temperature of structure WD2236+541 is found to be 22.42 K and 27.43 K respectively. The offset temperature of core is greater than 4 K. It indicates that the cavities are not in thermal equilibrium and have shorter life. The inclination angle of cavity is 54.2° . It means it is neither face on nor edge on. Total mass of dust structure in cavity is found to be 3×10^{25} kg. The correlation coefficient 0.54 indicates that data are correlated moderately. From the contour map of dust color temperature and dust mass, it is found that the cavity is homogenous and isotropic and follows the Cosmological Principle. The Gaussian distribution of dust color temperature indicates the cavity mostly shows symmetric behavior but mass shows asymmetric behavior i.e. polytropic in nature. It means the cavity is formed by external sources e.g. Pulsar, Supernova explosion etc. The size of cavity is $0.84 \text{ pc} \times 0.51 \text{ pc}$.

ACKNOWLEDGEMENT

We thank the editor and referee for the constructive comments and suggestions. One of the authors (BBS) thanks the University Grant Commission of Nepal for providing research funds and acknowledges the Central Department of Physics, T.U., Nepal for various kinds of support during Ph.D. In addition, we acknowledge the sky view virtual observatory (<http://skyview.gsfc.nasa.gov>), SIMBAD (<http://skyview.gsfc.nasa.gov>) for providing database and software.

REFERENCES

- [1] Palen S. *Schaum's Outlines of Astronomy*. USA: MC Graw Hill (2004).
- [2] Karttunen, H., Kroeger, P., Oja, H., Poutanen, M., Donner, K.J. *Fundamental Astronomy (5th Ed.)*. USA: Springer Berlin Heidelberg (2007).
- [3] Holberg, J.B., Oswalt, Terry D., & Sion, E.M. A determination of the Local density of White Dwarf Stars. *Astrophysical Journal*, 571, 512-518 (2002).

- [4] Schnee, S. L., Ridge, N.A., Goodman, A.A. Jason, G.L. A Complete Look at the Use of IRAS Emission Maps to Estimate Extinction and dust temperature *Astrophysical Journal*. 634,442-450 (2005).
- [5] Odenwald S. F. and Richard, L. J. Hydrodynamical Process in the Draco Molecular Cloud *Astrophysical Journal* 318 , 702-711 (1987).
- [6] Dupac, X., Bernard, J.P., Boudet, N., Giard, M., Lamarre, J.M., Meny, C., Pajot, F., Ristorcelli, I., Serra, G., Stepnik, B., Torre, J. P. Inverse temperature dependance of the dust submillimeter Spectral Index *Astronomy & Astrophysics*, 404, L11-L15 (2003).
- [7] Young, K., Philip, T.G.& Knapp, G.R. Circumstellar Shells Resolved in IRAS Survey Data .II. Analysis. *Astrophysical Journal*, 409, 725-738 (1993).
- [8] Holmberg E. On the apparent diameters and orientation in space of Extragalactic Nebulae. *Meddelanden fran Lunds Astronomiska Observation series II*, 117, 3-82 (1946).
- [9] Weinberg S. *Gravitation and Cosmology Principles and Application of General Theory of Relativity* . Newyork, London, Sydney, Toronto: John Willey and Sons (1972).